

Ergotropic advantage in a measurement-fueled quantum heat engine

Sidhant Jakhar* and Ramandeep S. Johal†

Department of Physical Sciences, Indian Institute of Science Education and Research Mohali, Sector 81, SAS Nagar, Manauli PO 140306 Punjab, India

This paper investigates a coupled two-qubits heat engine fueled by generalized measurements of the spin components and using a single heat reservoir as sink. Our model extends the four-stroke engine proposed by Yi and coworkers [Phys. Rev. E **96**, 022108 (2017)] by introducing an ergotropy-extracting stroke, resulting in a five-stroke cycle. For measurements along z-z directions, we find two possible occupation distributions that yield an active state and the ergotropic stroke improves the performance of the engine over the four-stroke cycle. Further, the three-stroke engine (without the adiabatic strokes) yields the same performance as the five-stroke engine. For arbitrary working medium and non-selective measurements, we prove that the total work output of a five-stroke engine is equal to the sum of the work outputs of the corresponding four-stroke and three-stroke engines. For measurement directions other than z-z, there may be many possible orderings of the post-measurement probabilities that yield an active state. However, as we illustrate for specific cases (x-x and x-z directions), a definite ordering is obtained with the projective measurements. Thus, we find that the five-stroke engine exploiting ergotropy outperforms both its four-stroke as well as three-stroke counterparts.

I. INTRODUCTION

Quantum thermodynamics [1–7], involves, amongst other pursuits, the study of thermal machines based on a quantum working medium. The idea of a quantum heat engine was first proposed by Scovil and Schulz-DuBois [8], who argued that a three-level maser, in simultaneous contact with a hot and a cold reservoir, can be regarded as a heat engine. State-of-the-art technology now allows us to experimentally control systems at the quantum scale, such as spins [9–14], superconducting qubits [15, 16] and trapped ions [17, 18]. So, the non-classical resources such as quantum entanglement, quantum coherence, quantum correlations and noise are being hotly pursued for their use in improving the performance of thermal machines away from the classical regime [19–28].

In recent years, quantum measurements [29, 30] have attracted increasing attention due to their ability to mediate energy exchange—either as work extraction [31] or as effective heat transfer. Measurement-induced energy injection can mimic the role of a hot reservoir, provided the measured observable does not commute with the system Hamiltonian [32–35]. Importantly, such engines operate without feedback control, distinguishing them from Szilard-type engines [36–38]. Related developments include quantum refrigerators and cooling protocols [39, 40], weak and continuous measurement schemes [41–43], non-ideal measurements [44] and work-fluctuation analyses [45]. Measurements further induce entropy production, probe–system correlations, and raise questions about associated energetic costs [46, 47]. The classification of measurement-induced energy exchange and its role as a fueling mechanism [48] remains an active research direction.

The present work extends the measurement-fueled engine [32, 33, 49] by using weak quantum measurements on a coupled-qubits system while exploiting the active nature of the post-measurement state of the system. We incorporate an ergotropy-extracting stroke [50–55] after the measurement stroke, thereby upgrading the four-stroke cycle into a five-stroke cycle. With measurements on the spin components along specific directions, we highlight the thermodynamic advantage of the ergotropic stroke by comparing the performance of five-stroke engine with the four-stroke (without ergotropy) as well as a three-stroke (without adiabatic strokes) cycle.

The paper is organized as follows. Section II describes the five-stroke heat cycle of the measurement-fueled engine, which is applied to a coupled qubits working medium in Section III A for z-z measurements, while comparing with four-stroke and three-stroke cycle in Section III B and III C respectively. Section IV describes the results for other measurement directions. Section V concludes the work with a summary and outlook.

II. FIVE-STROKE ENGINE

The working medium, or the system, is described by the Hamiltonian $H(B)$, with its initial state as the thermal state (ρ^{in}) corresponding to a heat reservoir at inverse temperature β , and the control parameter set at $B = B_2$. The occupation probability for the n -th energy eigenstate is labelled as p_n . The system undergoes a heat cycle consisting of five strokes, as described below (see also Fig. 1).

Stroke 1 → 2: This is a quantum adiabatic process (AP-1) in which the parameter B is increased from B_2 to B_1 sufficiently slowly such that the quantum adiabatic theorem [56] holds and the occupation probabilities remain unchanged.

Stroke 2 → 3: Keeping the Hamiltonian fixed at $H(B_1)$,

* ph20036@iisermohali.ac.in

† rsjohal@iisermohali.ac.in

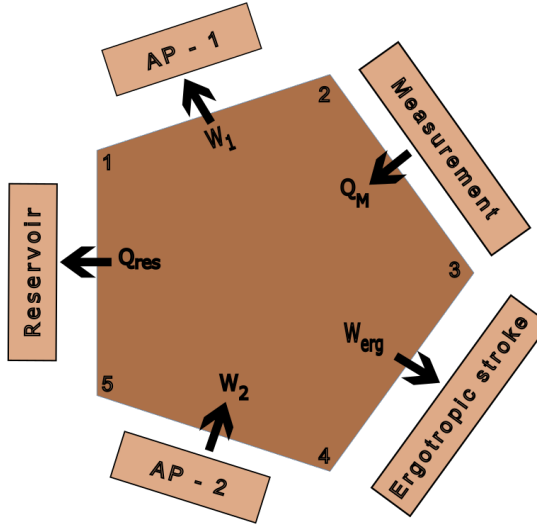


FIG. 1. A five-stroke engine cycle. $1 \rightarrow 2$ is the first adiabatic stroke. $2 \rightarrow 3$ is the measurement stroke. $3 \rightarrow 4$ is the ergotropy extraction stroke. $4 \rightarrow 5$ is the second adiabatic stroke. $5 \rightarrow 1$ is the thermalization stroke.

a generalized discrete measurement of an observable \mathcal{O} (incompatible with $H(B_1)$) is made. This measurement changes the state of the system, with the post-measurement occupation probabilities denoted as p_n^{PM} . Stroke $3 \rightarrow 4$: This is termed as the ergotropic stroke which is executed only if the post-measurement state is an active state [50]. In that case, ergotropy is the maximum work extracted from the system via a cyclic unitary evolution of its Hamiltonian.

Stroke $4 \rightarrow 5$: This is again a quantum adiabatic process (AP-2) in which the system is isolated and the parameter B is slowly brought back to its initial value B_2 .

Stroke $5 \rightarrow 1$: Finally, the system thermalizes with the heat reservoir and returns to the initial state, thus completing the cycle.

The exchange of heat or work in a stroke is defined as the difference of the final and the initial mean energy of the system during that stroke. The work in the AP-1 stroke is given by

$$W_1 = \sum_n [E_n(B_1) - E_n(B_2)] p_n. \quad (1)$$

The generalized measurement is characterized by the set of hermitian operators ($M_\alpha = M_\alpha^\dagger$) which satisfy the completeness relation $\sum_\alpha M_\alpha M_\alpha^\dagger = I$. The condition that these operators do not commute with the Hamiltonian $H(B_1)$ ensures that the measurement process adds energy (see Eq. (2)) to the system in the form of heat [32]. For a non-selective measurement where the outcomes are not recorded, the post-measurement state takes the form: $\rho^{\text{PM}} = \sum_\alpha M_\alpha \rho^{\text{in}} M_\alpha^\dagger$, with occupation probabilities over energy eigenstates are given by $p_n^{\text{PM}} = \langle \psi_n | \rho^{\text{PM}} | \psi_n \rangle$. The heat absorbed by the system in the measurement

stroke is then

$$Q_M = \sum_n E_n(B_1) [p_n^{\text{PM}} - p_n] > 0. \quad (2)$$

Suppose that after ergotropy extraction ($3 \rightarrow 4$), the system is left in a passive state ρ' with occupation probabilities p'_n . Then, the ergotropy is given by

$$W_{\text{erg}} = \sum_n E_n(B_1) [p'_n - p_n^{\text{PM}}] < 0. \quad (3)$$

Next, the work in the AP-2 stroke is

$$W_2 = \sum_n [E_n(B_2) - E_n(B_1)] p'_n. \quad (4)$$

Finally, the heat exchanged with the reservoir is

$$Q_{\text{res}} = \sum_n E_n(B_2) [p_n - p'_n]. \quad (5)$$

The sign of Q_{res} may be argued on thermodynamic grounds as follows. The state of the working medium or the system undergoes a cycle. The measurement step causes an increase in the entropy of the system while the adiabatic strokes keep the entropy unchanged. So, in order to return to initial state, the system must release heat/entropy to the reservoir, implying that $Q_{\text{res}} < 0$.

Using energy conservation, the total work extracted in a cycle is

$$W_T^{(5)} = -W_1 - W_2 - W_{\text{erg}} = Q_M + Q_{\text{res}}. \quad (6)$$

The operation of the engine requires $W_T^{(5)} > 0$. So, the efficiency is defined as

$$\eta = \frac{W_T^{(5)}}{Q_M}. \quad (7)$$

In the next section, we apply the above framework to a coupled qubits working medium where we consider spin measurements on each qubit, along specific directions.

III. COUPLED-QUBITS WORKING MEDIUM

We consider two coupled qubits following a 1D Hamiltonian with isotropic Heisenberg interaction:

$$H(B) = B(\sigma_z^A \otimes I^B + I^A \otimes \sigma_z^B) + 2J \sum_{i=x,y,z} \sigma_i^A \otimes \sigma_i^B. \quad (8)$$

The applied magnetic field (B) is the control parameter whereas the coupling strength $J > 0$ (anti-ferromagnetic case) is held fixed during the cycle. $I^{A,B}$ and $\sigma_i^{A,B}$ are the respective identity operator and Pauli matrices of the qubit A or B. We study the engine in the strong-coupling regime ($4J > B$) so that the energy eigenvalues in ascending order are $E_1 = -6J, E_2 = 2J - 2B, E_3 = 2J$

and $E_4 = 2J + 2B$, with $(|10\rangle - |01\rangle)/\sqrt{2} = |\psi_-\rangle$, $|11\rangle$, $(|10\rangle + |01\rangle)/\sqrt{2} = |\psi_+\rangle$ and $|00\rangle$ as the corresponding eigenstates. The initial state is $\rho^{\text{in}} = e^{-\beta H(B_2)}/Z$, where $Z = \sum_{n=1}^4 e^{-\beta E_n}$ is the partition function. Then, we have $p_n = e^{-\beta E_n}/Z$.

In the first adiabatic stroke, the work [Eq. (1)] is evaluated to be

$$W_1 = -2(B_1 - B_2)(p_2 - p_4) < 0. \quad (9)$$

Note that W_1 is independent of the measurement choice as it depends only on the initial state and the Hamiltonian $H(B)$.

We choose M_α operators in arbitrary directions \hat{n}^A and \hat{n}^B , in the following form:

$$\begin{aligned} M_{\pm, \pm} &= (c_0 I \pm c_1 \vec{\sigma}^A \cdot \hat{n}^A) \otimes (c_0 I \pm c_1 \vec{\sigma}^B \cdot \hat{n}^B), \\ M_{\pm, \mp} &= (c_0 I \pm c_1 \vec{\sigma}^A \cdot \hat{n}^A) \otimes (c_0 I \mp c_1 \vec{\sigma}^B \cdot \hat{n}^B), \end{aligned} \quad (10)$$

where c_0 and c_1 are real parameters. From the completeness relation: $2c_0^2 + 2c_1^2 = 1$. One of the parameters, say c_0 , can be chosen to define the strength of the measurement. Thus, $c_0 = c_1 = 1/2$ implies a strong or projective measurement [33]. The general expressions for the post-measurement probabilities are quite complicated and it is not feasible to determine the conditions for their relative ordering. So, in the following, we study measurements along specific directions.

A. z-z measurement

We choose $\vec{\sigma}^A \cdot \hat{n}^A = \sigma_z^A$ and $\vec{\sigma}^B \cdot \hat{n}^B = \sigma_z^B$. The post-measurement probabilities are given by

$$\begin{aligned} p_1^{\text{PM}} &= p_1 - 4c_0^2(1 - 2c_0^2)(p_1 - p_3), \\ p_2^{\text{PM}} &= p_2, \\ p_3^{\text{PM}} &= p_3 + 4c_0^2(1 - 2c_0^2)(p_1 - p_3), \\ p_4^{\text{PM}} &= p_4. \end{aligned} \quad (11)$$

The heat absorbed by the system during the measurement stroke [Eq. (2)] is

$$Q_M = 8J(p_3^{\text{PM}} - p_3) > 0. \quad (12)$$

As a result of the measurement, the occupation probabilities of levels E_2 and E_4 are unchanged, while those of E_1 and E_3 come closer to each other. Intuitively, we see that the post-measurement probability distribution becomes more uniform and so its Shannon entropy increases. Also, $p_1^{\text{PM}} - p_3^{\text{PM}} = (4c_0^2 - 1)^2(p_1 - p_3) \geq 0$, where the equality is obtained for $c_0 = 1/2$. Note that p_4 is still the lowest probability in the distribution (11) since the probabilities were initially ordered as $p_1 > p_2 > p_3 > p_4$. Based on these considerations, we can infer: $p_1^{\text{PM}} \geq p_3^{\text{PM}} > p_4$. However, to ascertain the active nature of the state ρ^{PM} , we have to determine the relative ordering of p_2 also. It

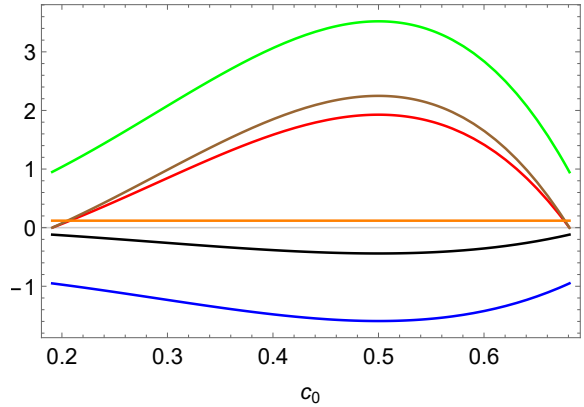


FIG. 2. R1 case: Q_M (green curve), W_{erg} (brown curve), W_T (red curve), W_1 (orange curve), W_2 (black curve) and Q_{res} (blue curve) vs. c_0 . Parameters are set at $B_2 = 3$, $J = 1$ and $\beta = 1$.

can be seen that an active post-measurement state implies one of the following two possibilities:

$$\begin{aligned} (\text{R1}) \quad p_1^{\text{PM}} &\geq p_3^{\text{PM}} > p_2 > p_4, \\ (\text{R2}) \quad p_2 &> p_1^{\text{PM}} \geq p_3^{\text{PM}} > p_4. \end{aligned}$$

Let us consider the R1 case in detail. Now, in the ergotropy stroke, the occupation probabilities p_n^{PM} get re-ordered in an opposite sense to the energy eigenvalues [50], implying that $p'_1 = p_1^{\text{PM}}$, $p'_2 = p_3^{\text{PM}}$, $p'_3 = p_2$ and $p'_4 = p_4$. Thus, the system state after the ergotropy stroke can be given as

$$\begin{aligned} \rho' &= p_1^{\text{PM}} |\psi_-\rangle \langle \psi_-| + p_3^{\text{PM}} |11\rangle \langle 11| + p_2 |\psi_+\rangle \langle \psi_+| \\ &\quad + p_4 |00\rangle \langle 00|. \end{aligned} \quad (13)$$

Note that R1 case is characterized by the condition $p_3^{\text{PM}} > p_2$, which can be cast in the form:

$$4c_0^2(1 - 2c_0^2) > \frac{e^{2\beta B_2} - 1}{e^{8\beta J} - 1} = \chi(B_2, J, \beta), \quad (14)$$

which implies that R1 case bounds the parameter c_0 as follows: $(1 - \sqrt{1 - 2\chi})/4 < c_0^2 < (1 + \sqrt{1 - 2\chi})/4$, where $\chi < 1/2$.

Next, the ergotropy [Eq. (3)] is given by

$$W_{\text{erg}} = -2B_1(p_3^{\text{PM}} - p_2) < 0. \quad (15)$$

Work in the second adiabatic stroke [Eq. (4)] is

$$W_2 = 2(B_1 - B_2)(p_3^{\text{PM}} - p_4) > 0. \quad (16)$$

Finally, the heat exchange in the thermalization stroke [Eq. (5)] is

$$Q_{\text{res}} = 2B_2(p_3^{\text{PM}} - p_2) - 8J(p_3^{\text{PM}} - p_3). \quad (17)$$

Using Eq. (11), we can show that $Q_{\text{res}} < 0$, as required. The net work extracted is

$$W_T^{(5)} = Q_M + Q_{\text{res}} = 2B_2(p_3^{\text{PM}} - p_2) > 0. \quad (18)$$

In Fig. 2, the above heat and work contributions are plotted for a specific example. It is observed that the work output becomes optimal at $c_0 = 1/2$ i.e. when p_3^{PM} achieves its maximum value $(p_1 + p_3)/2$. The efficiency in the R1 case can be expressed as

$$\eta = \frac{B_2}{4J} \left[1 - \frac{(e^{2\beta B_2} - 1)}{4c_0^2(1 - 2c_0^2)(e^{8\beta J} - 1)} \right]. \quad (19)$$

It is interesting to note that η is independent of the parameter B_1 . This is not a generic feature, but depends on the energy spectrum. For the given model, η is maximum at $c_0 = 1/2$ i.e. for projective measurements. The efficiency is plotted in Fig. 3. For a given c_0 , η increases with β . For low enough temperatures, η grows rapidly with c_0 and approaches its limiting value $B_2/4J$. In Fig. 4, the efficiency is plotted versus J for a fixed c_0 at various temperatures. Again, decreasing the temperature increases the efficiency at low J values, while for large J values, all efficiency curves merge into each other and goes to zero at very large J .

Similarly, we can study the R2 case which is characterized by the ordering: $p_2 > p_1^{\text{PM}} \geq p_3^{\text{PM}} > p_4$. To appreciate how this ordering may come about, consider the difference: $p_2 - p_1^{\text{PM}} = (p_2 - p_1) + 4c_0^2(1 - 2c_0^2)(p_1 - p_3)$. As we are working in the regime $4J > B_2$, so B_2 close to $4J$ implies that the lowest two levels are close to each other. Then, the term $(p_2 - p_1)$ will be negligible and the condition $p_2 > p_1^{\text{PM}}$ can prevail, thereby producing the R2 case.

The total work output is

$$W_T^{(5)} = 2(4J - B_2)(p_2 - p_1^{\text{PM}}) > 0, \quad (20)$$

whereas Q_M is given by Eq. (12). The efficiency of this case can then be computed. As shown in Fig. 5, the R2 case yields a rather small efficiency. Another notable feature is that upon decreasing the temperature, the efficiency decreases, thus showing an opposite trend to the R1 case.

B. Four-stroke cycle

For comparison, we also consider the four-stroke cycle [32, 33] that does not involve the ergotropic stroke. It implies the occupation probabilities in AP-2 are given by p_n^{PM} . The expressions for heat and work in different stages can be obtained by replacing each p'_n with p_n^{PM} in the expressions for the five-stroke cycle as in Sec. II. Thus, the total work extracted can be expressed as:

$$W_T^{(4)} = \sum_n [E_n(B_2) - E_n(B_1)](p_n - p_n^{\text{PM}}). \quad (21)$$

For the two-qubits system and with z-z measurements, we obtain So, the net work output of the four-stroke cycle is zero. This feature was noted in Ref. [33] for z-z projective measurements and we affirm it for generalized

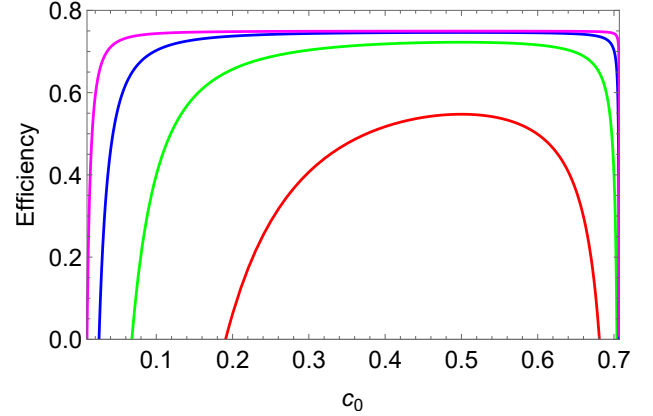


FIG. 3. R1 case: Efficiency [Eq. (19)] vs. $c_0 \in [0, 1/\sqrt{2}]$. Red curve ($\beta = 1$), green curve ($\beta = 2$), blue curve ($\beta = 3$) and magenta curve ($\beta = 4$). Here, $B_2 = 3$ and $J = 1$. So, the limiting value of the efficiency (as $\beta \rightarrow \infty$) is $B_2/4J = 0.75$.

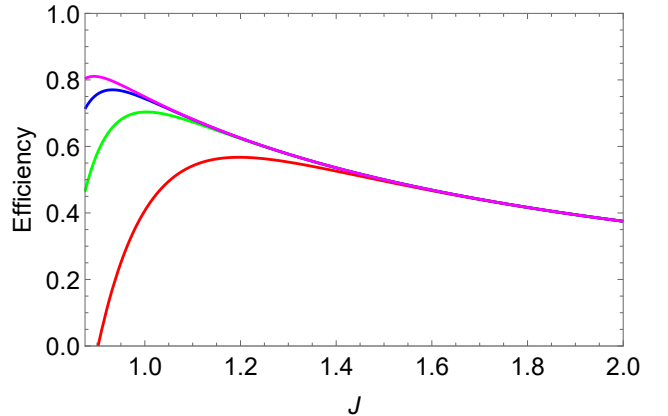


FIG. 4. R1 case: Efficiency [Eq. (19)] vs. J . Red curve ($\beta = 1$), green curve ($\beta = 2$), blue curve ($\beta = 3$) and magenta curve ($\beta = 4$). Here, $B_2 = 3$ and $c_0 = 0.3$.

measurements too. Thus, we can conclude that the ergotropy stroke improves the performance of the engine based on generalized z-z measurements.

C. Three-stroke cycle

As an alternative, we consider an ergotropy based three-stroke cycle consisting of the following steps. We prepare the system with Hamiltonian $H(B_2)$ in a thermal state ρ^{in} at inverse temperature β . i) The system is isolated from the reservoir (assuming a weak interaction with the reservoir and so negligible costs in attaching and detaching the system from the reservoir) and non-selective generalized measurements are performed which transform the state to ρ^{PM} . ii) Ergotropy, W_{erg} , is extracted which yields the passive state ρ' . iii) Finally, the system is brought to the initial state by thermalization with the reservoir. The net work extracted, equal in

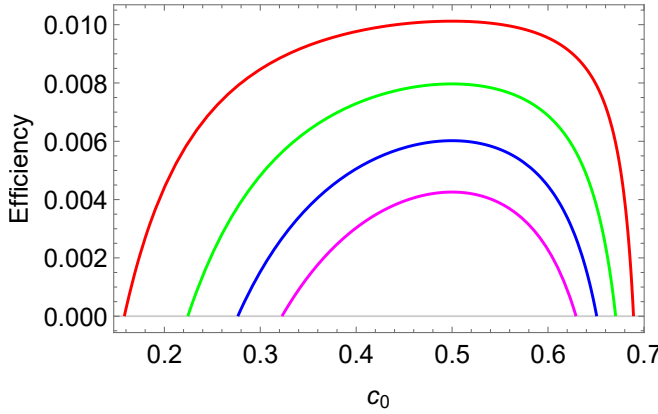


FIG. 5. R2 case: Efficiency vs. c_0 . Red curve ($\beta = 1$), green curve ($\beta = 2$), blue curve ($\beta = 3$) and magenta curve ($\beta = 4$). $B_2 = 3.9$, $J = 1$. The efficiency decreases as the temperature is lowered at a given measurement strength, unlike the R1 case (see Fig. 3). The R2 efficiency is also maximized at $c_0 = 1/2$.

magnitude to the ergotropy in step (ii), is given by

$$W_T^{(3)} = -W_{\text{erg}} = \sum_n E_n(B_2)(p_n^{\text{PM}} - p'_n). \quad (22)$$

From Eqs. (6), (21) and (22), we obtain an interesting equality:

$$W_T^{(5)} = W_T^{(4)} + W_T^{(3)}. \quad (23)$$

Note that the above relation holds for arbitrary Hamiltonian and nonselective measurements. It implies that the performance of a four-stroke measurement engine ($W_T^{(4)} \geq 0$), with an active post-measurement state, can be enhanced by using the five-stroke cycle.

For the R1 case, we obtain $W_T^{(3)} = 2B_2(p_3^{\text{PM}} - p_2)$, which, as expected, is equal to the work in the five-stroke cycle [Eq. (18)] since $W_T^{(4)} = 0$ for z-z measurements. Q_M for the three-stroke cycle is also given by Eq. (12). Therefore, its efficiency is the same as for the five-stroke cycle [Eq. (19)]. A similar conclusion holds for the case R2.

IV. OTHER MEASUREMENT DIRECTIONS

We have also studied the performance of the engine with generalized measurements along x-x (y-y), x-y, and x-z (y-z) directions. Usually, for these cases, there are many possibilities for ordering the post-measurement probabilities. To illustrate, we consider x-x measurements for which we set $\vec{\sigma}^A \cdot \hat{n}^A = \sigma_x^A$ and $\vec{\sigma}^B \cdot \hat{n}^B = \sigma_x^B$ in Eq. (10). The post-measurement probabilities are given

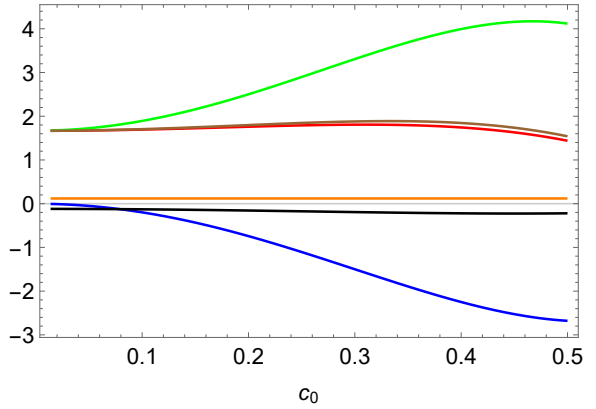


FIG. 6. x-x case: Q_M (green curve), W_{erg} (brown curve), W_T (red curve), W_1 (orange curve), W_2 (black curve) and Q_{res} (blue curve). $B_1 = 3.5$, $B_2 = 3$, $J = 1$ and $\beta = 1$.

by

$$\begin{aligned} p_1^{\text{PM}} &= 4c_0^4 p_1 + 4c_1^4 p_1 + 4c_0^2 c_1^2 (p_2 + p_4), \\ p_2^{\text{PM}} &= 4c_0^4 p_2 + 4c_1^4 p_4 + 4c_0^2 c_1^2 (p_1 + p_3), \\ p_3^{\text{PM}} &= 4c_0^4 p_3 + 4c_1^4 p_3 + 4c_0^2 c_1^2 (p_2 + p_4), \\ p_4^{\text{PM}} &= 4c_0^4 p_4 + 4c_1^4 p_2 + 4c_0^2 c_1^2 (p_1 + p_3). \end{aligned} \quad (24)$$

The relative ordering of the above probabilities is not straightforward, though we can prove specific inequalities, such as $p_1^{\text{PM}} > p_3^{\text{PM}}$. For $c_0 < 1/2$, $p_2^{\text{PM}} < p_4^{\text{PM}}$ ($p_2^{\text{PM}} > p_4^{\text{PM}}$ for $c_0 > 1/2$). For the purpose of illustration, we consider one of the orderings, given by $p_1^{\text{PM}} > p_4^{\text{PM}} \geq p_2^{\text{PM}} > p_3^{\text{PM}}$, in the range $0 < c_0 \leq 1/2$. Firstly, unlike the case of z-z measurements, we have a non-zero total work for the four-stroke cycle with weak measurements. Heat and work involved are shown in Fig. 6. In Fig. 7, we show the effect of weak measurements as they can lead to a higher efficiency compared to projective measurements. The efficiency is plotted versus J (Fig. 8) for a fixed c_0 to show the effect of the reservoir temperature and we note that the efficiency reduces with the lowering of the temperature. In the special case of x-x projective measurements ($c_0 = c_1 = 1/2$), Eqs. (24) simplify as

$$\begin{aligned} p_1^{\text{PM}} &= \frac{1}{4} + \frac{p_1 - p_3}{4}, \\ p_2^{\text{PM}} &= p_4^{\text{PM}} = \frac{1}{4}, \\ p_3^{\text{PM}} &= \frac{1}{4} - \frac{p_1 - p_3}{4}, \end{aligned} \quad (25)$$

The heat exchange during the measurement stroke is

$$Q_M = 2B_1(p_2 - p_4) + 2J(2p_1 - p_2 - p_4). \quad (26)$$

The above probability distribution follows a definite ordering: $p_1^{\text{PM}} > p_2^{\text{PM}} = p_4^{\text{PM}} > p_3^{\text{PM}}$, and indicates an active state. The ergotropy is given by $W_{\text{erg}} =$

$-B_1(p_1 - p_3)/2 < 0$, while the total work output is

$$W_T^{(5)} = 2(B_1 - B_2)(p_2 - p_4) + \frac{B_2}{2}(p_1 - p_3) > 0. \quad (27)$$

Compared to the above, the work output of a four-stroke cycle with projective measurements is while the three-stroke cycle yields $W_T^{(3)} = B_2(p_1 - p_3)/2$. Thus, we verify the equality (23).

Similarly, for the x-z projective measurements, we have a definite ordering i.e. $p_2^{\text{PM}} > p_1^{\text{PM}} = p_3^{\text{PM}} (= 1/4) > p_4^{\text{PM}}$ which describes an active state. Now, the heat exchange during the measurement stroke is

$$Q_M = B_1(p_2 - p_4) + 2J(3p_1 - p_2 - p_3 - p_4), \quad (28)$$

while the total work output is

$$W_T^{(5)} = (B_1 - B_2)(p_2 - p_4) + \frac{1}{2}(4J - B_2)(p_2 - p_4). \quad (29)$$

The first and the second terms on the rhs above can be identified with $W_T^{(4)}$ and $W_T^{(3)}$ respectively. Thus, we conclude that the projective measurements yield a higher work as well as efficiency for the five-stroke cycle than the corresponding four-stroke cycle.

For the case of x-y projective measurements, we find that the post-measurement probability distribution is uniform ($p_n^{\text{PM}} = 1/4$). Being a passive state, the ergotropic stroke does not help in this case.

Before closing this section, we remark on the case of spin-measurements along arbitrary directions. As mentioned earlier, relations between post-measurement probabilities are hard to obtain here. However, if we restrict ourselves to the projective measurements, the following inequality always holds.

$$p_2^{\text{PM}} - p_4^{\text{PM}} = \frac{1}{2}(\cos^2 \theta_A + \cos^2 \theta_B)(p_2 - p_4) \geq 0. \quad (30)$$

The equality $p_2^{\text{PM}} = p_4^{\text{PM}}$ is recovered for projective measurements in xy -plane for each qubit ($\theta_A = \theta_B = \pi/2$) irrespective of the angles ϕ_A and ϕ_B . On the other hand, for z-z measurements ($\theta_A = \theta_B = 0$), we obtain $p_2^{\text{PM}} = p_2$ and $p_4^{\text{PM}} = p_4$, as found in Section III A.

V. SUMMARY

In this paper, we have studied a measurement-fueled quantum engine based on a coupled two-qubits system where weak measurements of the spin components are used as a source of heat. In the specific cases we have analyzed, the z-z case yields zero work output in the four-stroke cycle with generalized measurements. There are two possible orderings of the post-measurement probabilities which correspond to active post-measurement state ρ^{PM} . Incorporating an ergotropy-extracting stroke after the measurement stroke yields a positive work output.

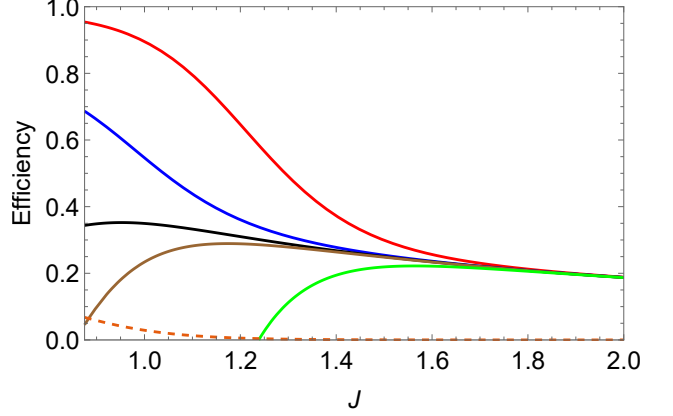


FIG. 7. x-x case: Efficiency vs. J for five-stroke engine. Red curve ($c_0 = 0.1$), blue curve ($c_0 = 0.3$), black curve ($c_0 = 0.5$), brown curve ($c_0 = 0.6$), green curve ($c_0 = 0.7$). For comparison, the efficiency of a four-stroke engine with projective measurement of Ref. [33] (dashed curve) is also plotted. Here, $B_1 = 3.5$, $B_2 = 3$, and $\beta = 1$.

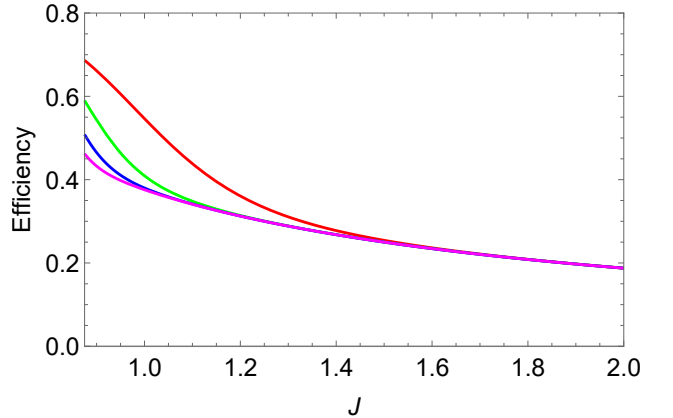


FIG. 8. x-x case: Efficiency vs. J . Red curve ($\beta = 1$), green curve ($\beta = 2$), blue curve ($\beta = 3$) and magenta curve ($\beta = 4$). $B_1 = 3.5$, $B_2 = 3$ and $c_0 = 0.3$.

Furthermore, a reduced three-stroke cycle (without adiabatic strokes) yields the same performance as the five-stroke cycle.

For measurement directions, such as x-x or x-z, the four-stroke cycle produces non-zero work, and the ergotropic extension further improves the performance. In general, several orderings of the post-measurement probabilities may occur, although projective measurements can yield a unique ordering. Notably, weak x-x and x-z measurements within a five-stroke cycle can achieve a higher efficiency than projective measurements, underscoring the role of weak measurements in optimizing the performance of a quantum engine.

ACKNOWLEDGMENTS

S.J. thanks Sachin Sonkar for useful discussions and acknowledges financial support in the form of Senior Re-

search Fellowship from the Indian Institute of Science education and Research Mohali.

[1] S. Vinjanampathy and J. Anders, Quantum thermodynamics, *Contemporary Physics* **57**, 545 (2016).

[2] F. Binder, L. A. Correa, C. Gogolin, J. Anders, and G. Adesso, eds., *Thermodynamics in the Quantum Regime: Fundamental Aspects and New Directions*, Fundamental Theories of Physics, Vol. 195 (Springer, Cham, 2019).

[3] G. Mahler, *Quantum Thermodynamic Processes: Energy and Information Flow at the Nanoscale (1st ed.)* (Jenny Stanford Publishing, Singapore, 2014).

[4] S. Campbell, I. D’Amico, M. A. Ciampini, J. Anders, N. Ares, S. Artini, A. Auffèves, L. B. Oftelie, L. P. Bettmann, M. V. S. Bonança, T. Busch, M. Campisi, M. F. Cavalcante, L. A. Correa, E. Cuestas, C. B. Dag, S. Dago, S. Deffner, A. D. Campo, and A. D.-O. et al., Roadmap on quantum thermodynamics (2025), arXiv:2504.20145 [quant-ph].

[5] R. Alicki, The quantum open system as a model of the heat engine, *Journal of Physics A: Mathematical and General* **12**, L103 (1979).

[6] T. D. Kieu, The second law, Maxwell’s demon, and work derivable from quantum heat engines, *Phys. Rev. Lett.* **93**, 140403 (2004).

[7] A. E. Allahverdyan, R. S. Johal, and G. Mahler, Work extremum principle: Structure and function of quantum heat engines, *Phys. Rev. E* **77**, 041118 (2008).

[8] H. E. D. Scovil and E. O. Schulz-DuBois, Three-level masers as heat engines, *Phys. Rev. Lett.* **2**, 262 (1959).

[9] W. Hübner, G. Lefkidis, C. D. Dong, D. Chaudhuri, L. Chotorlishvili, and J. Berakdar, Spin-dependent Otto quantum heat engine based on a molecular substance, *Phys. Rev. B* **90**, 024401 (2014).

[10] J. P. S. Peterson, T. B. Batalhão, M. Herrera, A. M. Souza, R. S. Sarthour, I. S. Oliveira, and R. M. Serra, Experimental characterization of a spin quantum heat engine, *Phys. Rev. Lett.* **123**, 240601 (2019).

[11] R. J. de Assis, T. M. de Mendonça, C. J. Villas-Boas, A. M. de Souza, R. S. Sarthour, I. S. Oliveira, and N. G. de Almeida, Efficiency of a quantum Otto heat engine operating under a reservoir at effective negative temperatures, *Phys. Rev. Lett.* **122**, 240602 (2019).

[12] K. Ono, S. N. Shevchenko, T. Mori, S. Moriyama, and F. Nori, Analog of a quantum heat engine using a single-spin qubit, *Phys. Rev. Lett.* **125**, 166802 (2020).

[13] J. Nettersheim, S. Burgardt, Q. Bouton, D. Adam, E. Lutz, and A. Widera, Power of a quasispin quantum Otto engine at negative effective spin temperature, *PRX Quantum* **3**, 040334 (2022).

[14] S. Sonkar and R. S. Johal, Spin-based quantum Otto engines and majorization, *Phys. Rev. A* **107**, 032220 (2023).

[15] B. Karimi and J. P. Pekola, Otto refrigerator based on a superconducting qubit: Classical and quantum performance, *Phys. Rev. B* **94**, 184503 (2016).

[16] M. A. Aamir, P. Jamet Suria, J. A. Marín Guzmán, C. Castillo-Moreno, J. M. Epstein, N. Yunger Halpern, and S. Gasparinetti, Thermally driven quantum refrigerator autonomously resets a superconducting qubit, *Nature Physics* **21**, 318 (2025).

[17] G. Maslennikov, S. Ding, R. Hablitzel, J. Gan, A. Roulet, S. Nimmrichter, J. Dai, V. Scarani, and D. Matsukevich, Quantum absorption refrigerator with trapped ions, *Nature Communications* **10**, 202 (2019).

[18] O. Abah, J. Roßnagel, G. Jacob, S. Deffner, F. Schmidt-Kaler, K. Singer, and E. Lutz, Single-ion heat engine at maximum power, *Phys. Rev. Lett.* **109**, 203006 (2012).

[19] A. Hewgill, A. Ferraro, and G. De Chiara, Quantum correlations and thermodynamic performances of two-qubit engines with local and common baths, *Phys. Rev. A* **98**, 042102 (2018).

[20] K. Funo, Y. Watanabe, and M. Ueda, Thermodynamic work gain from entanglement, *Phys. Rev. A* **88**, 052319 (2013).

[21] R. Alicki and M. Fannes, Entanglement boost for extractable work from ensembles of quantum batteries, *Phys. Rev. E* **87**, 042123 (2013).

[22] K. V. Hovhannisyan, M. Perarnau-Llobet, M. Huber, and A. Acín, Entanglement generation is not necessary for optimal work extraction, *Phys. Rev. Lett.* **111**, 240401 (2013).

[23] M. Perarnau-Llobet, K. V. Hovhannisyan, M. Huber, P. Skrzypczyk, N. Brunner, and A. Acín, Extractable work from correlations, *Phys. Rev. X* **5**, 041011 (2015).

[24] K. Korzekwa, M. Lostaglio, J. Oppenheim, and D. Jennings, The extraction of work from quantum coherence, *New Journal of Physics* **18**, 023045 (2016).

[25] J. Goold, M. Huber, A. Riera, L. d. Rio, and P. Skrzypczyk, The role of quantum information in thermodynamics—a topical review, *Journal of Physics A: Mathematical and Theoretical* **49**, 143001 (2016).

[26] J. Klatzow, J. N. Becker, P. M. Ledingham, C. Weinzel, K. T. Kaczmarek, D. J. Saunders, J. Nunn, I. A. Walmsley, R. Uzdin, and E. Poem, Experimental demonstration of quantum effects in the operation of microscopic heat engines, *Phys. Rev. Lett.* **122**, 110601 (2019).

[27] G.-F. Zhang, Entangled quantum heat engines based on two two-spin systems with Dzyaloshinski-Moriya anisotropic antisymmetric interaction, *The European Physical Journal D* **49**, 123 (2008).

[28] R. Dassonneville, C. Elouard, R. Cazali, R. Assouly, A. Bienfait, A. Auffèves, and B. Huard, Amplifying microwave pulses with a single qubit engine fueled by quantum measurements (2025), arXiv:2501.17069 [quant-ph].

[29] K. Jacobs, *Quantum Measurement Theory and its Applications* (Cambridge university press, Cambridge, 2014).

[30] M. A. Nielsen and I. L. Chuang, *Quantum computation and quantum information* (Cambridge university press, Cambridge, 2010).

[31] T. Opatrný, A. Misra, and G. Kurizki, Work generation from thermal noise by quantum phase-sensitive observation, *Phys. Rev. Lett.* **127**, 040602 (2021).

- [32] J. Yi, P. Talkner, and Y. W. Kim, Single-temperature quantum engine without feedback control, *Phys. Rev. E* **96**, 022108 (2017).
- [33] A. Das and S. Ghosh, Measurement based quantum heat engine with coupled working medium, *Entropy* **21**, 10.3390/e21111131 (2019).
- [34] M. F. Anka, T. R. de Oliveira, and D. Jonathan, Measurement-based quantum heat engine in a multilevel system, *Phys. Rev. E* **104**, 054128 (2021).
- [35] X. Linpeng, N. Piccione, M. Maffei, L. Bresque, S. P. Prasad, A. N. Jordan, A. Auffèves, and K. W. Murch, Quantum energetics of a noncommuting measurement, *Phys. Rev. Res.* **6**, 033045 (2024).
- [36] L. Szilard, über die entropieverminderung in einem thermodynamischen system bei eingriffen intelligenter wesen, *Zeitschrift für Physik* **53**, 840 (1929).
- [37] S. W. Kim, T. Sagawa, S. De Liberato, and M. Ueda, Quantum Szilard engine, *Phys. Rev. Lett.* **106**, 070401 (2011).
- [38] H. S. Leff and A. F. Rex, *Maxwell's Demon 2: Entropy, classical and quantum information, computing* (IOP Publishing, Bristol, 2004).
- [39] L. Buffoni, A. Solfanelli, P. Verrucchi, A. Cuccoli, and M. Campisi, Quantum measurement cooling, *Phys. Rev. Lett.* **122**, 070603 (2019).
- [40] C. Elouard, S. K. Manikandan, A. N. Jordan, and G. Haack, Revealing the fuel of a quantum continuous measurement-based refrigerator (2025), arXiv:2502.10349 [quant-ph].
- [41] K. Jacobs and D. A. Steck, A straightforward introduction to continuous quantum measurement, *Contemporary Physics* **47**, 279–303 (2006).
- [42] A. E. Allahverdyan, R. Balian, and T. M. Nieuwenhuizen, Understanding quantum measurement from the solution of dynamical models, *Physics Reports* **525**, 1 (2011).
- [43] L. B. Ferraz and C. Elouard, Weak continuous measurements require more work than strong ones (2025), arXiv:2502.09732 [quant-ph].
- [44] A. Panda, F. C. Binder, and S. Vinjanampathy, Nonideal measurement heat engines, *Phys. Rev. A* **108**, 062214 (2023).
- [45] T. Debarba, G. Manzano, Y. Guryanova, M. Huber, and N. Friis, Work estimation and work fluctuations in the presence of non-ideal measurements, *New Journal of Physics* **21**, 113002 (2019).
- [46] K. Jacobs, Quantum measurement and the first law of thermodynamics: The energy cost of measurement is the work value of the acquired information, *Phys. Rev. E* **86**, 040106 (2012).
- [47] C. L Latune and C. Elouard, A thermodynamically consistent approach to the energy costs of quantum measurements, *Quantum* **9**, 1614 (2025).
- [48] L. Bresque, P. A. Camati, S. Rogers, K. Murch, A. N. Jordan, and A. Auffèves, Two-qubit engine fueled by entanglement and local measurements, *Phys. Rev. Lett.* **126**, 120605 (2021).
- [49] N. Behzadi, Quantum engine based on general measurements, *Journal of Physics A: Mathematical and Theoretical* **54**, 015304 (2020).
- [50] A. E. Allahverdyan, R. Balian, and T. M. Nieuwenhuizen, Maximal work extraction from finite quantum systems, *Europhysics Letters* **67**, 565 (2004).
- [51] G. Francica, J. Goold, F. Plastina, and M. Paternostro, Daemonic ergotropy: enhanced work extraction from quantum correlations, *npj Quantum Information* **3**, 12 (2017).
- [52] T. Biswas, M. Łobejko, P. Mazurek, K. Jałowiecki, and M. Horodecki, Extraction of ergotropy: free energy bound and application to open cycle engines, *Quantum* **6**, 841 (2022).
- [53] A. Touil, B. Çakmak, and S. Deffner, Ergotropy from quantum and classical correlations, *Journal of Physics A: Mathematical and Theoretical* **55**, 025301 (2021).
- [54] M. Hadipour and S. Haseli, Work extraction from quantum coherence in non-equilibrium environment, *Scientific Reports* **14**, 24876 (2024).
- [55] J. M. Z. Choquehuanca, P. A. C. Obando, M. S. Sarandy, and F. M. de Paula, Ergotropy-based quantum thermodynamics (2025), arXiv:2504.07200 [quant-ph].
- [56] M. Born and V. Fock, Beweis des adiabatensatzes, *Zeitschrift für Physik* **51**, 165 (1928).